A98-31654 ICAS-98-5,9,1

COMPRESSION AFTER IMPACT BEHAVIOUR OF MULTILAYER WOVEN GLASS/VINYL ESTER COMPOSITES

M. Bannister
Cooperative Research Centre for Advanced Composites Structures
Melbourne, Victoria, Australia

P. Callus
DSTO – Aeronautical and Maritime Research Laboratories
Melbourne, Victoria, Australia

I. Herszberg
The Sir Lawrence Wackett Centre for Aerospace Design Technology
Royal Melbourne Institute of Technology
Melbourne, Victoria, Australia

Abstract

The impact performance of E-glass reinforced composite materials was examined. A number of 2D and 3D weave architectures were tested and their compression-after-impact (CAI) properties were related to their weave architecture. It was found that there was no significant difference in the impact resistance of the various materials, however the impact tolerance was very dependant upon the weave architecture. Highly crimped weave architectures and those containing through-thickness reinforcement were observed to give the best impact tolerance. One of the 3D weaves investigated was observed to have an improvement in CAI strength of up to 50% over a 2D weave typical of those used in aerospace composite structures.

Introduction

Fibre reinforced polymer materials have a number of advantages when used as components for the aerospace industry. Due to their high strength-to-weight and stiffness-to-weight ratios and their fatigue and corrosion resistance it is possible to manufacture components that demonstrate significant weight savings and improved life-time performance over that of metal parts. Glass and carbon fibre reinforced polymers are widely used as secondary structures, however the use of composites, particularly in primary structure, is being limited by their high cost of production and their poor resistance to impact damage. This sensitivity to impact is essentially due to the two-dimensional architecture of fibre reinforcement in the plane of most composite structures which leads to an inherent weakness in the thickness direction.

An incident such as a dropped tool or stone impact can cause delamination between the plies thus resulting in a significant drop in strength of the component. The lack of impact tolerance arises from the fact that unlike metallic structures, laminate structures only have a limited amount of elastic and plastic deformation and so impact energy is dissipated through mechanisms such as matrix cracking, fibre-matrix debonding, surface micro-buckling, fibre shear-out, fibre fracture and delamination. This danger is further exacerbated by the fact that some of these damage features caused by low energy impacts may not be visible on the impact surface and so may be missed by routine inspections.

By using advanced technologies that have been developed in the textile weaving industry, it is possible to produce multilayer, structural preforms that have a three-dimensional (3D) fibre architecture, i..e. one in which the orientation of fibres at any point is not restricted to a plane, as is the case with traditional reinforcement fabrics for composite manufacture[1]. A liquid moulding process may then be used to impregnate the preform with resin. This production method can be a highly automated process and has the potential to produce low cost, reliable composite structural components of complex shapes. Most importantly, as a result of the 3D nature of the fibre architecture, such structures are less prone to delamination and thus their impact resistance is increased significantly[1-5].

A large variety of three-dimensional fibre architectures can produced but not all of these may be suitable for composite structures as any increase in the proportion of through-the-thickness (TTT) reinforcement (or binders) leads to a corresponding decrease in the amount of in-plane fibres[6-8]. This will reduce the in-plane, undamaged mechanical performance of the component. Although the damage tolerance of the three-dimensional woven composite will be improved, due to this reduction of the in-plane compressive properties the end result may be an overall reduction of the composites' structural performance. It is therefore of significant importance that an understanding be gained of the relationship between the 3D weave architecture and the mechanical

21st ICAS Congress
13-18 September 1998
Melbourne, Australia

performance of the resultant composite, particularly under impact loads.

Experimental

Specimen Production

Three different weave architectures were produced for this investigation and the results for compression-after-impact strength analysed along with results from previous investigations[9]. Firstly a commercially available, 8-harness satin-weave fabric made from 300 tex glass yarn was obtained. This fabric is typical of that used in the aerospace industry and 13 layers were needed in a 0°/90° layup to produce the required panel thickness of approximately 3 mm. Two further weave architectures were produced on an electronically controlled jacquard loom similar to that used in the textile industry. These fabrics consisted of (i) a 6 warp layer, 3D weave with a layer-to-layer angle interlock binder pattern and (ii) a 6 warp layer 2D plain weave, woven to resemble the 3D woven fabric but without the binder yarns. Both of the fabrics manufactured on the jacquard loom were produced using 900 tex E-glass warp yarns, 825 tex E-glass weft yarns and 275 tex E-glass binder yarns. An idealised schematic of the 3D weave is shown in Figure 1.

All of these 3 fabrics were consolidated with Derakane 411-C50 vinyl ester resin using resin transfer moulding techniques in a heated press. A press pressure of 1500kPa was used to ensure a uniform specimen thickness of 3 mm and post-curing was conducted at 120°C for 2 hours. The fibre volume fractions of these three materials were measured by the Loss-on-Ignition technique (ASTM D2584-94) and are shown in Table 1.

The previous fabrics investigated consisted of the same 8-harness satin weave fabric and a 6 warp layer, 3D weave with an orthogonal binder architecture. The 3D weave was produced on a 24 shaft mechanical dobby handloom using 1200 tex E-glass warp and weft yarns and a 68 tex E-glass binder yarn. This difference in the weight of the E-glass yarns used resulted in the composite panel being thicker than those produced on the jacquard loom (3.8mm as compared to 3.0mm). However, in order to compare their relative impact performance, the relevant data was normalised with respect to the specimen thickness and fibre volume fraction of yarn in the testing direction. An idealised schematic of the orthogonal structure is shown in Figure 2.

Both fabrics had been consolidated with Ciba-Geigy GY260 epoxy resin by resin transfer moulding at a cure temperature of 80°C. This epoxy resin and the vinyl ester resin had similar mechanical performance and, as will be seen from the data presented, resulted in practically identical impact performance for the satin weave specimens. The fibre volume fraction of the consolidated orthogonal specimen is recorded in Table 1.

Testing

Compression-after-impact specimens were machined to dimensions of 90 × 115 mm with the warp yarns oriented in the load direction. The coupons were damaged using a drop-weight impact rig shown in Figure 3. Two different impact weights of 400 and 1100 grams, dropped from heights ranging from 300 to 3000 mm were used to generate impact energies of up to 29 J using a hemi-spherical impact head of 12.7 mm diameter. Impact was always administered in the centre of the coupon. Incident and rebound velocities of the impactor were measured using a light sensor connected to a data logger.

Due to the translucency of the glass/resin specimens it was possible to measure the damage area after impact by transmitted light methods. The impacted specimens were placed on a light box and the damage area, characterised by a change in translucency, was measured. Selected specimens were also assessed using ultrasonic methods but it was found that this technique underestimated the damage area formed by the impact.

Compression testing was performed on a 100kN MTS servo hydraulic testing machine using the compression-after-impact rig shown in Figure 4. The test specimens were supported by anti-buckling face plates to prevent gross buckling of the specimens. These were secured with just enough force to prevent the coupons from buckling but not so much as to hinder movement in the loading axis. In order to prevent interference with the protruding impact damage and to allow visual inspection of the damage zone, a circular window 40 mm in diameter was cut into the faceplates. Specimens were loaded at 0.5 mm/min until failure.

Results and Discussion

Consolidated architecture

Micrographs of the resulting weave architectures after consolidation by RTM are presented in Figures 5-8. The satin weave (Figure 5) showed a fairly uniform structure as a result of the fine weight of the plies, and views from both the warp and weft directions were virtually indistinguishable. There was no evidence of porosity seen from the micrographs.

The 2-D plain weave, shown in Figure 6a. with the warp yarns travelling into the page, displayed large resin rich channels between adjacent warp tows but only moderate crimping of the weft yarns. In Figure 6b. the warp tows,

which are in the plane of the page, are extremely crimped and resin rich channels can be clearly seen to separate each weft tow in a diagonal fashion. Although not evident in the micrographs, the resin rich channels progress very far into the depth when viewed through a stereoscopic microscope.

The 3-D multi weave shows the greatest deviation from the ideal architecture shown previously in Figure 1. The 3-D binder architecture can be seen in Figure 7a., together with large resin rich channels caused by bunching of the tows. In Figure 7b. it can be clearly seen that the warp yarns are significantly crimped. This is due to the presence of the binder yarns which, because of frictional effects during the weaving process, exert a compressive force on the warp tows, causing them to crimp. The maximum misalignment angles of the warp or load bearing tows in the 2-D plain weave and 3-D weave were measured and the results summarised in Table 2. Although both the plain and 3D weaves had similar average misalignment angles, the 3D weave had a much higher maximum misalignment angle. Misalignment angles for the satin weave were not calculated because of difficulty in tracing each individual tow.

By way of comparison, the micrographs of the orthogonal structure produced on the dobby loom are shown in Figure 8. It is clear from this figure that the warp and weft yarns in this structure suffer little or no crimping. This is due to the fact that this material was woven by hand on the dobby loom and thus a greater degree of control was possible over the manufacturing process. This allowed the effect of friction on the binder yarns to be minimised and resulted in a structure that had very straight warp and weft yarns. The average and maximum misalignment angles for the orthogonal weave were therefore recorded as zero degrees.

Impact behaviour

Specimens were impacted at energies ranging from 1 to 29 J using a drop weight impactor and the resultant damage area was measured by transmitted light. It was found that there was very little difference between the damage areas formed in each of the weave architectures across the entire impact energy range. The damage area was approximately circular at low impact energies but transformed to a more diamond shape at higher impact energies.

A plot of compression-after-impact strength against impact energy is shown in Figure 9. It is clear that the best impact performance is given by the older, orthogonal weave architecture manufactured on the dobby hand loom. The satin weave specimens produced the next best impact performance with the specimens manufactured from both the epoxy resin and the vinyl ester resin having practically identical measured strengths. The worst performance was observed in the 3D weave and plain weave specimens manufactured on the jacquard loom.

Both the orthogonal and satin weave specimens failed by delamination buckling, an example of which is shown in Figure 10a. However, for the 3D weave and the plain weave specimens, shear failure was the dominant mechanism, as shown in Figures 10b. and 10c.

The reason for the variation in the compression-after-impact strength of the specimens described here is thought to be related to the differences in their weave architectures. The satin weave material had no discernable difference in impact resistance from the other materials tested, which is indicated by the size of the damage area formed for the same impact energy. However, the steep gradient of the compression-after-impact versus impact energy curve indicates that the satin weave material has poor impact tolerance, that is, a low ability to maintain its strength after impact has occurred.

The satin weave fabric has a very fine structure with the yarns relatively uncrimped, hence this material has good compression properties in the undamaged state. However, the very planar nature of the fabric means that there is very little fibre reinforcement in the thickness direction, therefore little resistance to delaminations being formed and growing under the application of a compressive load. This situation is demonstrated by the dramatic reduction in the material's compression strength after impact damage has occurred. Even at very small impact energy levels, delaminations will grow under compressive load, allowing the delaminated plies to act independently of each other and hence cause the material to fail through delamination buckling (Figure 10a.). At higher energies, the CAI response of the satin weave begins to exhibit an asymptotic behaviour and this may be attributable to a saturation of impact damage in the specimen.

Both the plain weave and 3D weave materials had very similar CAI performance. Although their undamaged strengths were very low due to the highly crimped nature of the weave architecture, the reduction in CAI strength was relatively small over the entire energy range therefore the impact tolerance of the materials is very good. This improved impact tolerance is thought to be the result of the highly crimped nature of the weave architectures which has allowed shear failure to occur. Under the action of a compressive load, the crimped yarns try to rotate and therefore set up a shear stress at the boundary of the yarns. Failure is then governed by the shear strength of the interface at the boundary between the tow and the matrix.

Unfortunately, there is a natural "fault-line" running perpendicular to the regions of maximum tow misalignment in the plain weave material and, to a slightly lesser extent, the 3D weave material (shown in Figure 11). This "fault-line" is composed of the fine resin rich channels running in between the tows. When the shear stress created at the fibre/matrix interface exceeds that for the matrix, fracture propagates easily through the "fault-line". As shown in Figure 11, failure of the specimen does not need to involve fracture of the fibres, failure of the interface is sufficient to cause failure in the specimen. The fact that the compressive strength of the composite is dominated by the ease of fracture propagation through this natural "fault-line" may explain the reason for the gradual drop in CAI strength with increasing impact energy. Damage upon impact would only aid in decreasing CAI strength by introducing defects into the interface and hence decreasing interfacial shear strength.

As mentioned previously, the best impact performance was produced by the older, orthogonal weave. This material had very good undamaged compression strength due to the uncrimped load carrying yarns. However, Figure 7 demonstrates that the impact tolerance of the orthogonal structure to be better than the satin weave material, as evidenced by the ability to carry significantly larger compression loads even at high impact energies. For example, at impact energies of roughly 6 J/mm, the CAI strength of the orthogonal material was approximately 50% greater than the satin weave. Although the impact resistance of the two materials was comparable, the improved impact tolerance is thought to be a direct result of the presence of the binder yarns. These yarns will hinder the propagation of delaminations under the action of the compressive loads and thus cause failure through delamination buckling to occur at higher loads than with the satin weave material.

Conclusion

The impact performance of composite materials reinforced with E-glass was examined. Four different styles of weave architecture were tested; (i) 8 harness satin weave fabric typical of that used in the aerospace industry, (ii) 3D weave (layer interlock structure) produced on an automated jacquard loom, (iii) Plain weave similar to the 3D weave but without through thickness binder yarns, and (iv) Orthogonal 3D weave produced on a hand dobby loom.

It was found that the weave architecture had a significant effect on the impact performance of the various materials. Although all the specimens had comparable impact resistance (measured by damage area produced at the same impact energy) the satin weave had poor impact tolerance in that the compression strength dropped dramatically as the impact energy increased. This is due to the lack of through-thickness reinforcement. The 3D and plain weave specimens had very good impact tolerance but poor overall compression strengths due to the highly crimped nature of the weave architectures promoting premature shear failure. The best impact performance was produced by the orthogonal weave. Its compression strength was naturally high due to the uncrimped nature of the load carrying yarns and it had superior impact tolerance to the satin weave (up to 50% improvement) due to the presence of the binder yarns.

The outcome of these tests show that it is possible to change the impact performance of composite materials through the creation of weave architectures that contain fibre reinforcement in the thickness direction. This reinforcement may be in the form of increased yarn waviness or binder yarns which travel in the thickness direction. Both of these options hinder the propagation between the layers of load carrying yarns of delaminations formed upon impact and thus delaying the onset of failure. However, as has been observed in these tests, a change to the weave can also be detrimental to the impact performance. The severe crimp that was produced in the plain weave and 3D weave specimens resulted in a reduction of the CAI strength due to the promotion of an alternate failure mode. Clearly a greater understanding is needed of the relationship between the weave architecture and the impact properties of the composites before materials can be designed with specific impact performance

References

1. Arendts, F.J., Drechsler, K, Brandt, J., "Manufacturing and mechanical performance of composites with 3-D woven fibre reinforcement", 4th Textile Structural Composites Symposium, Philadelphia, July 1989.
2. Dickinson, L., Mohammed, M. H., Klang, E., "Impact resistance and compressional properties of three-dimensional woven carbon/epoxy composites", ECCM-4, Sept. 25-28, 1990, Stuttgart, Germany, Elsevier, eds. Fuller, Grüninger, Schulte, Bunsell, Massiah, pp 659 – 664.
3. Ding Y.Q., Wenger W., McIlhagger R., "Structural characterisation and mechanical properties of 3-D woven composites", European SAMPE 1993, pp 1 – 9.
4. Farley G. L., Smith B. T., Maiden J., "Compressive response of thick layer composite laminates with through-the-thickness reinforcement", Journal of Reinforced Plastics and Composites, Vol 11, July 1992, pp 787-810.

5. Brandt J., Drechsler K., Mohamed M. & Gu P., "Manufacture and performance of carbon/epoxy 3-D woven composites", 37th International SAMPE Symposium, 9-12 March 1992, pp 864-877.

6. Kozey V., Kumar S., Adanur S. & Mohamed H., "Compressive failure in 2-D and 3-D woven and laminated glass/epoxy composites", 50 Years Progress in Materials and Science Technology International SAMPE Technical Conference, Vol. 26, 1994, pp 315-325.

7. Cox B., Dadkah M., Morris W. & Flintoff J., "Failure mechanisms of 3D woven composites in tension, compression and bending", Acta Metallurgical Materials, 1994, Vol. 42, 12, pp 3967-3984.

8. Chou S., Chen H-C. & Chen H-E., "Effect of weave structure on mechanical fracture behaviour of three-dimensional carbon fibre fabric reinforced epoxy resin composites", Composites Science and Technology, 45, 1992, pp 23-35.

9. Camporeale S., "Mechanical testing of multilayer woven composites", AV408 Thesis, 1995, Department of Aerospace Engineering, Royal Melbourne Institute of Technology. Melbourne, Australia.

Specimen Architecture	Fibre volume (%)
Satin weave	53
2-D Plain weave	64
3-D Multi weave	67
Orthogonal	62

Table 1. Measured fibre volume of the various architectures

Material	Average misalignment angle	Maximum. Misalignment angle
2-D Plain weave	8.1°	21.0°
3-D weave	8.5°	31.4°
Orthogonal	0°	0°

Table 2. Warp tow misalignment angles

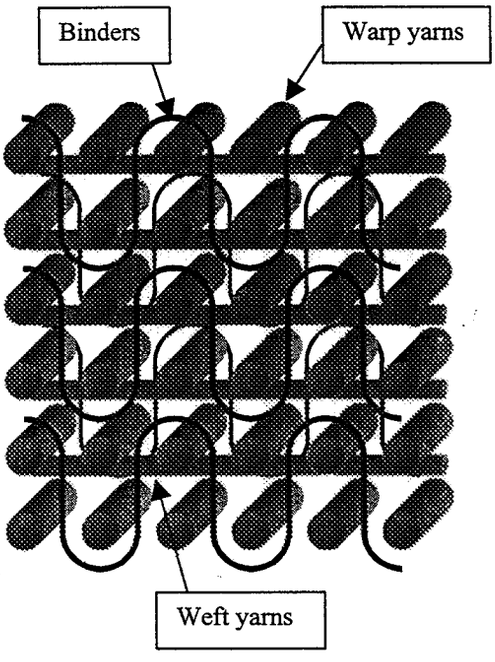

FIGURE 1 – 3D Weave architecture

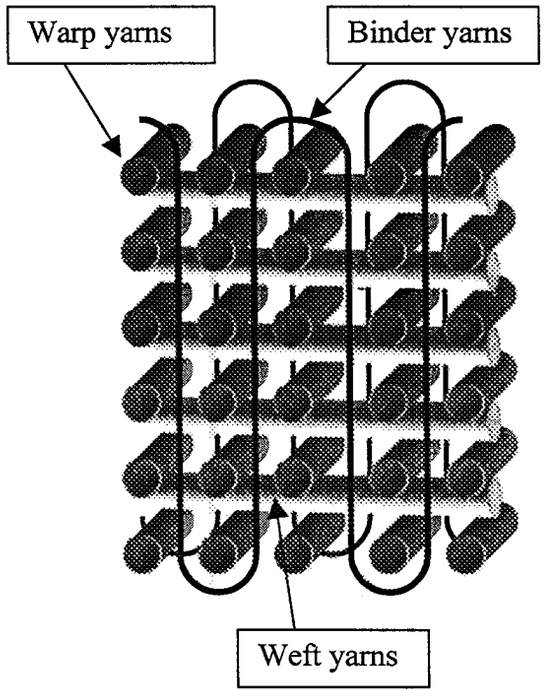

FIGURE 2 – Orthogonal architecture

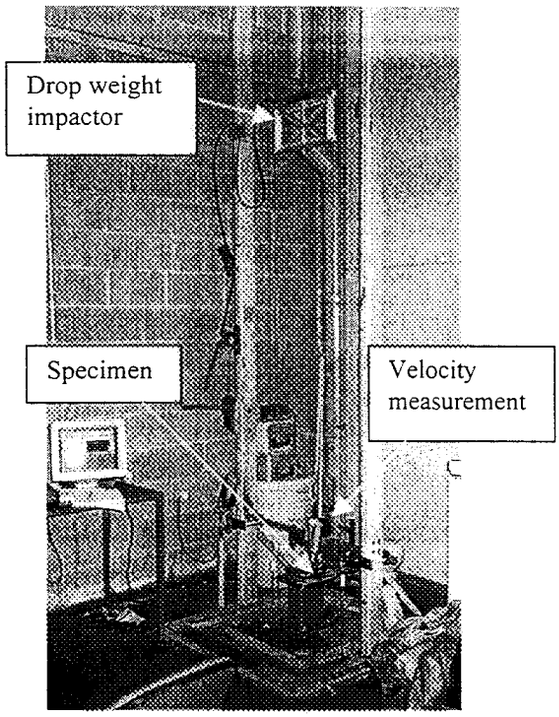

FIGURE 3 – Drop weight impact rig

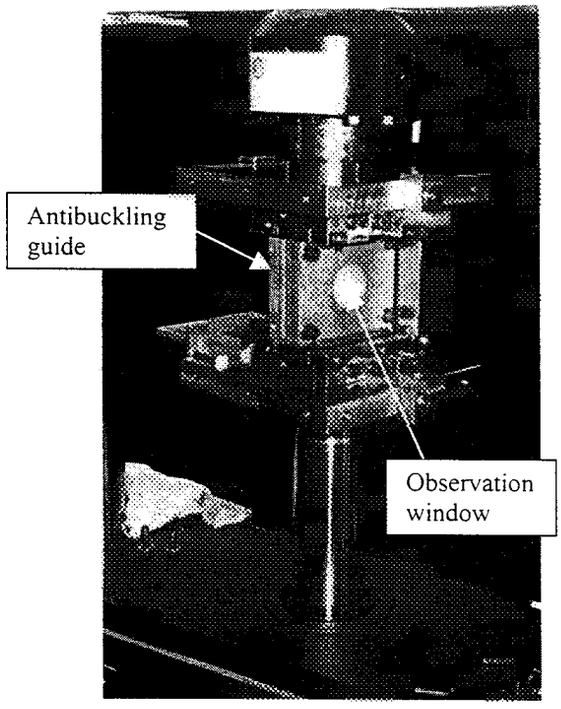

FIGURE 4 – Compression-after-impact rig

FIGURE 5 – Satin weave architecture

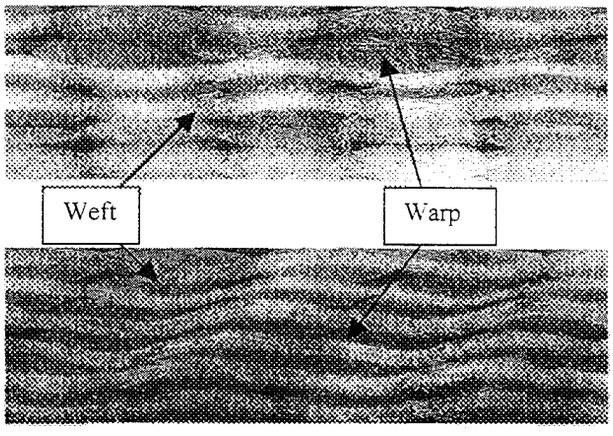

FIGURE 6 – Plain weave. Top a) warp into page
Bottom b) weft into page

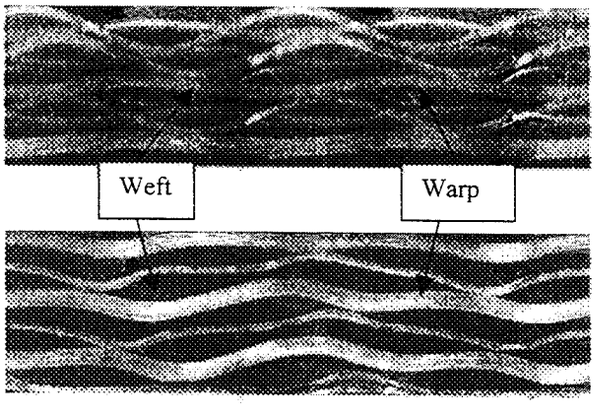

FIGURE 7 – 3D weave. Top a) warp into page
Bottom b) weft into page

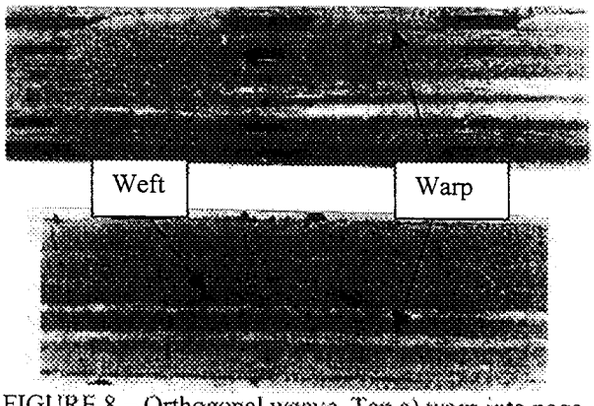

FIGURE 8 – Orthogonal weave. Top a) warp into page
Bottom b) weft into page

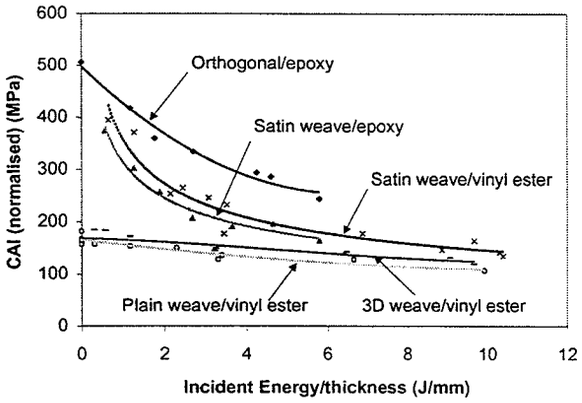

FIGURE 9 – CAI strength versus impact energy

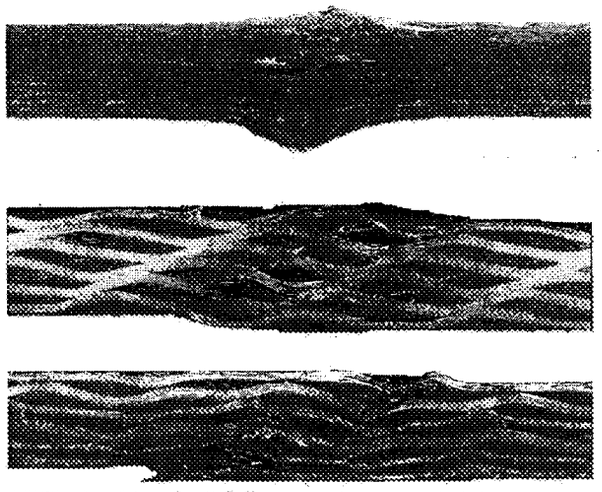

FIGURE 10 – CAI failure modes. Top a) delamination buckling in satin weave. Middle b) shear failure in plain weave. Bottom c) shear failure in 3D weave

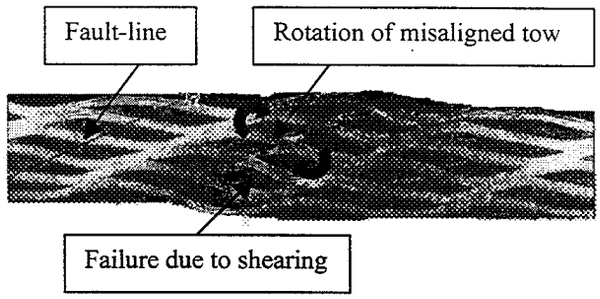

FIGURE 11 – Illustration of "fault-line" causing shear failure.